Biotechnic & Histochemistry

ISSN: 1052-0295 (Print) 1473-7760 (Online) Journal homepage: www.tandfonline.com/journals/ibih20

Morphological characterization of 3D cell cultures generated by liquid overlay technique

W. Metzger, E. Oh, L. Lemke, M. Hannig, F. Krull, S. Antonyuk & T. Pohlemann

To cite this article: W. Metzger, E. Oh, L. Lemke, M. Hannig, F. Krull, S. Antonyuk & T. Pohlemann (2025) Morphological characterization of 3D cell cultures generated by liquid overlay technique, Biotechnic & Histochemistry, 100:8, 494-504, DOI: 10.1080/10520295.2025.2568063

To link to this article: https://doi.org/10.1080/10520295.2025.2568063

Published online: 16 Oct 2025.

BIOTECHNIC & HISTOCHEMISTRY
2025, VOL. 100, NO. 8, 494–504
https://doi.org/10.1080/10520295.2025.2568063

Taylor & Francis
Taylor & Francis Group

Morphological characterization of 3D cell cultures generated by liquid overlay technique

W. Metzger [a], E. Oh [a], L. Lemke [b], M. Hannig [b], F. Krull [c], S. Antonyuk [c], and T. Pohlemann [a]

[a]Department of Trauma, Hand and Reconstructive Surgery, Saarland University, Homburg, Germany; [b]Department of Operative Dentistry, Periodontology and Preventive Dentistry, Saarland University, Homburg, Germany; [c]Institute of Particle Process Engineering, University of Kaiserslautern-Landau (RPTU), Kaiserslautern, Germany

ABSTRACT

Cultivating cells in 3D is considered a significant advancement in cell culture models, as it better reflects natural cellular environments compared to 2D cultures. However, analytical methods like standard light microscopy are less effective for 3D cultures. In this study, 3D cell cultures were generated using the liquid overlay technique with 10,000, 50,000, 100,000 and 200,000 Normal Human Dermal Fibroblasts, analyzed on days 1, 2, and 3 post-seeding. We quantified the influence of fixation with paraformaldehyde or glutardialdehyde/dehydration on their morphology compared to living 3D cell cultures. They were analyzed by light microscopy, scanning electron microscopy as well as by digital light microscopy (height profile measurement). Over time, the cultures decreased in size, likely due to cell shrinkage and structural reorganization. The size reduction could be mathematically described by an exponential decay function. The proportion of round spheroids versus indented aggregates depended on cell number, culture age, and fixation method. On day 1, cultures seeded with 10,000 cells formed nearly 100% round spheroids, regardless of fixation. Higher cell numbers led to fewer round spheroids, and fixation further reduced their number. This suggests that large cell quantities sediment in layers due to steric hindrance, forming indentations. Since aldehydes are responsible for cross-linking proteins, we hypothesize that this chemical reaction, combined with low stability of the 3D cell cultures, leads to the increased formation of the indented 3D cell aggregates. This is consistent with an overall increase in the number of round spheroids and a decrease of the negative influence of fixation over time. In summary, it is important to consider the number of seeded cells, the incubation time, as well as the possible fixation effects when generating stable spheroids using the liquid overlay technique for down-stream experiments.

KEYWORDS

3D cell aggregates; age; fixation; indentation; morphology; scanning electron microscopy; spheroids

Introduction

Adherently growing cells have been cultivated in 2D as monolayers on artificial surfaces, e.g. polystyrene for decades, which led to a tremendous increase in knowledge and a huge range of medical applications. However, it is nowadays generally accepted that 2D cell culture models have limitations and reflect the physiological growth of cells in tissues insufficiently. This insight was aptly formulated by Fitzgerald and co-workers: "Life in 3D is never flat and cell culture should not be either" (Fitzgerald et al. 2015). Accordingly, 3D cell culture models are therefore regarded to be superior to 2D cell culture models bearing the potential to bridge the gap between 2D cell cultures and natural tissues (Efremov et al. 2021; Saraswathibhatla et al. 2023). Many differences encountered by a direct comparison of 2D and 3D cultures have been described in the literature (Grässer et al. 2018; Metzger et al. 2021). Due to the great medical importance, only differences in sensitivity to cytostatic drugs will be mentioned here (Unger et al. 2014). Consequently, 3D cell culture models are often used in the pharmaceutical testing of new promising compounds (Zanoni et al. 2019). Moreover, 3D cell cultures are used in angiogenesis-related research (Heiss et al. 2015), as well as for evaluating cell-surface interactions (Metzger et al. 2017). They are also discussed as building blocks for tissue-engineering approaches (Laschke and Menger 2017). However, 3D cell cultures have also found their way into biomechanical studies. Although much is already known about the biomechanics of single cells, 3D cell cultures allow for the study of interactions with neighboring cells and the extracellular matrix. Many methods are used to quantify the biomechanics of 3D cell cultures, such as parallel plate compression, nanoindentation, osmo-mechanical stress,

CONTACT W. Metzger johann-wolfgang.metzger@uks.eu Department of Trauma, Hand and Reconstructive Surgery, Saarland University, Building 57, Homburg 66421, Germany

and micropipette aspiration (Efremov et al. 2021). These methods have one thing in common: a force deforms the 3D cell culture, providing insight into the biomechanics and, ultimately, the quantification of Young's modulus. Clearly, the morphology, size, and cellular composition of the 3D cell cultures strongly influence the outcome of such experiments. In summary, 3D cell culture models can be considered as an ideal bridge between 2D in vitro studies and in vivo animal studies, supporting the 3 R principle (replacement, reduction, refinement, Bloise et al. 2024).

It is therefore not surprising that the number of publications per year on 3D cell culture listed in PubMed has increased exponentially from the late 1960s until today. In 2020 alone, approximately 1200 new publications were listed (Jensen and Teng 2020). However, there is a catch: the handling of 3D cultures is more difficult compared to 2D cell cultures and the possibilities for microscopic analysis are limited (Grässer et al. 2018). Many different techniques to generate spheroids of adherently growing cells from a single cell suspension have been described (Achilli et al. 2012). Methods based on scaffold-free techniques using a self-assembly mechanism of the cells are of particular interest, because the resulting spheroids initially consist only of cells, but subsequently begin to synthesize extracellular matrix components within the spheroid (Rescigno et al. 2021). Our group has identified the liquid overlay technique (LOT) as a versatile technique that allows for easy and highly reproducible generation of spheroids after overnight incubation. The LOT has been successfully used to generate mono- and co-cultures of up to three different cell types (Metzger et al. 2011; Dorst et al. 2014; Jennewein et al. 2016). In all cases, one spheroid per well was formed overnight and showed an almost round morphology already on the first day. As mentioned above, the microscopic analysis of spheroids is limited and only little information could be obtained considering the 3D morphology of the spheroids. For the purpose of this study, we used the term "3D cell cultures" prior to their detailed classification as round "spheroids" or clearly indented "3D cell aggregates." Accordingly, the aim of this study was a detailed analysis of the morphology of 3D cell cultures consisting of different numbers of Normal Human Dermal Fibroblasts (NHDF) depending on their age. We quantified the development of the size of vital 3D cell cultures over time and described it by a mathematical formula. The results of the light microscopic analysis of the morphology were compared with the results of scanning electron microscopy (SEM). In addition to the analysis of vital 3D cell cultures, we also tested the influence of fixation with paraformaldehyde (PFA) and glutardialdehyde (GDA)/dehydration. PFA fixation is our standard fixation procedure for immunostaining of 2D cell cultures (Metzger et al. 2014) or sections of spheroids (Jennewein et al. 2016). Fixation of cellular samples with GDA followed by dehydration is our standard preparation of biological samples for SEM analysis in our laboratory (Später et al. 2022).

Materials and methods

Cell culture

Juvenile NHDF were isolated from the foreskin of an 8-year-old boy and were purchased at passage 2 from a commercial supplier (lot 394Z023, PromoCell GmbH, Heidelberg, Germany). Cells were expanded in Dulbecco's modified Eagle's medium (DMEM, Sigma-Aldrich, Taufkirchen, Germany) supplemented with 15% fetal calf serum (PanBiotech, Aidenbach, Germany) under standard cell culture conditions (37°C, 95% humidity, 5% CO_2). Standard trypsinization procedures were used to detach cells in confluent layers. At passage 4, NHDF were frozen as cryo-cultures (500,000 cells/cryo vial) in Cryo-SFM freezing medium (PromoCell) as a master cell bank.

Liquid overlay technique

Prior to the generation of 3D cell cultures, NHDF were expanded as described above to obtain the required number of cells. After the NHDF were detached, the cell number was determined using a hemocytometer. The LOT has already been described in detail (Metzger et al. 2011). Similar to other methods for generating 3D cell cultures, the principle of LOT is to prevent adherent cells from attaching to a cell culture surface. For this purpose, the cavities of 96-well flat-bottomed plates (Greiner Bio-One, Frickenhausen, Germany) were coated with cell-repellent agarose (1% in distilled water). The concentration of cells was adjusted to give a total of 10,000, 50,000, 100,000, and 200,000 cells in a volume of 100 µl per well. Since the agarose coating prevented the cells from adhering to the bottom of the wells, the NHDF adhered to each other and formed exactly one spheroid in which all seeded cells self-organized into a 3D structure overnight, as already shown (Metzger et al. 2017). We analyzed the 3D cell cultures on days 1, 2, and 3 after seeding the cell suspension into the cavities of the 96-well plates.

Development of size of spheroids and mathematical description

For each experiment (n = 5), photomicrographs of 15 vital 3D cell cultures of each size and time point were taken using a Nikon Eclipse TS100 phase-contrast microscope (objective 10x/0.25, Ph1 ADL, Nikon Cooperation, Tokyo, Japan) and a Sony Cybershot 3.0 digital camera (Sony Corporation, Tokyo, Japan). Photomicrographs were analyzed using the image processing software Image J (National Institutes of Health, Bethesda, MD, USA). For each 3D cell culture, the minimum and maximum diameters were measured, and the average of the two diameters was calculated:

$$d_{average} = \frac{d_{max} + d_{min}}{2} \quad (1)$$

Morphology of 3D cell cultures

The aim of the morphological analysis of the 3D cell cultures obtained was to quantify the number and ratio between round spheroids without and 3D aggregates with a bright central indention, whose appearance is reminiscent of shrimp crackers or donuts. After seeding in agarose coated wells, the morphology of 3D cell cultures (vital and after fixation with PFA or GDA/dehydration) was analyzed from day 1 to day 3. Additionally, the morphology of GDA-fixed spheroids was imaged by SEM.

Vital 3D cultures

The 3D cultures in the agarose coated cavities of 96-well plates were thoroughly analyzed by transmitted light microscopy (Nikon Eclipse TS100). If the 3D cultures showed signs of a brighter central region compared to the peripheral region, they were not classified as spheroids but as 3D aggregates. Similarly, only 3D cell cultures with a dark central region were classified as spheroids. We investigated whether a brighter central region of vital 3D cell cultures correlates with a non-spherical morphology or not. Therefore, the samples were additionally analyzed using a Keyence VHX 5000 digital light microscope at a final magnification of 200x (Keyence, Osaka, Japan). After manually defining the lowest and highest points of the 3D cell cultures, a z-stack was automatically recorded and a height profile measurement was performed.

PFA-fixed 3D cell cultures

PFA (Carl Roth GmbH & Co KG, Karlsruhe, Germany) was dissolved in phosphate-buffered saline (PBS) to a final concentration of 4%. The 3D cell cultures were harvested using piston-operated pipettes in combination with low retention pipette tips. After sedimentation via a short run in a microcentrifuge (Carl Roth GmbH & Co KG), the cell culture medium was removed and the 3D cell cultures were washed in PBS. Then the samples were incubated for 15 min at room temperature with continuous agitation to prevent the samples from sticking together. Finally, the PFA-fixed 3D cell cultures were transferred to PBS and the number of 3D cell cultures was quantified with a Leica Wild M420 stereo microscope (Leica, Wetzlar, Germany) as follows: samples with visible indentations were referred to as 3D aggregates; samples that appeared round and had no indentations were referred to as spheroids.

GDA-fixed 3D cell cultures

GDA-fixation was performed according to our standardized SEM preparation protocol for biological samples. The 3D cell cultures were harvested and washed as described above. The samples were fixed for 10 min at room temperature with continuous agitation in GDA (2 vol%; Science Services GmbH, Munich, Germany) in 0.1 M sodium cacodylate buffer (pH 7.4; Carl Roth GmbH & Co KG, Karlsruhe, Germany). The fixative solution was removed, and the 3D cell cultures were washed three times with 0.1 M sodium cacodylate buffer, followed by dehydration in an ascending ethanol series (70 vol%, 80 vol%, 90 vol%, 96 vol%, and 100 vol%). Finally, dehydration was completed by washing the samples in a mixture (50:50) of 100 vol% ethanol and hexamethyldisilazane (HMDS; Carl Roth GmbH Co KG), followed by another incubation in pure HMDS. Dehydration was completed by covering the spheroids with pure HMDS, which evaporated completely overnight. The next day, the 3D cell cultures were transferred to conductive adhesive tabs on standard SEM pin stubs (Micro to Nano, Haarlem, Netherlands). To allow for the SEM-observation, the 3D cell cultures were first sputtered with carbon (SCD 030, Balzers Union, Balzers, Liechtenstein) followed by additional sputtering with gold (3x for 60s with gold (SCD 005, Balzers Union)) in order to reduce charging of the samples. Evaluation of the morphology was performed using a FEI XL 30 ESEM FEG SEM (FEI, Hillsboro, OR, USA) under high vacuum conditions at an acceleration voltage of 5 kV in the secondary electrons mode.

The morphology of a subset of these GDA-fixed 3D cell aggregates was analyzed as already described for the PFA-fixed samples without transfer to conductive adhesive tabs and final sputtering.

Statistical analysis

All numerical results presented in this study are means with standard deviations. Differences were tested for significance ($p < 0.05$) by one-way ANOVA followed by a Student-Neuman-Keuls test for post-hoc analysis using SigmaPlot software version 13.0 (Systat Software Inc., Paola Alto, CA, USA). If the normality test (Shapiro-Wilk) or the equal variance test failed, the Kruskal-Wallis one-way analysis of variance on ranks was used to determine significant differences between the results and, if significance was found, the Student-Neuman-Keuls post-hoc analysis was used.

Results

Performance of the LOT

As previously described by our group, LOT is a simple and cost-effective method to generate standardized 3D cell cultures with high reproducibility (Metzger et al. 2011, 2021). Irrespective of the total number of cells seeded per well, which ranged from 10,000 to 200,000, exactly one 3D cell culture was formed after an overnight incubation (Figure 1).

All seeded cells were integrated into a well-defined 3D cell culture with a regular, almost round morphology. Only 3D cell cultures with the highest cell number of 200,000 per well resulted in more irregular morphologies that persisted until day 2 (Figure 1K). It is also worth mentioning that these 3D cell cultures on days 1 and 2 (Figure 1J, K) exceeded the dimensions of the field of view of our microscope even at the lowest magnification and only the diameter that could be detected without a doubt was used.

For 3D cell cultures consisting of 10,000 cells, no bright central region could be seen at all, but the 3D cell cultures became darker with time. Only a few of the

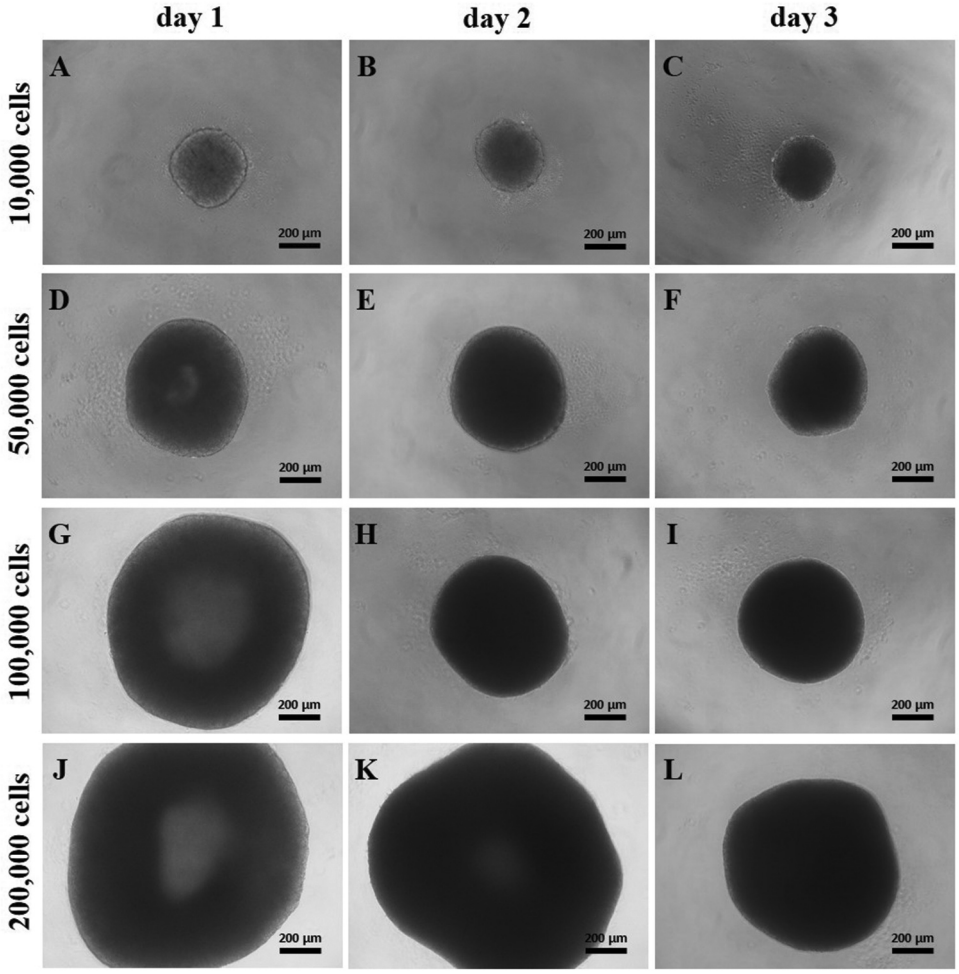

Figure 1. Photomicrographs of living 3D cell cultures (phase contrast) on day 1 (A, D, G, J), day 2 (B, E, H, K), and day 3 (C, F, I, L) after seeding into agarose-coated wells of 96-well plates. 10,000 cells (A–C), 50,000 cells (D–F), 100,000 cells (G–I), and 200,000 cells (J–L) were seeded. A continuous reduction in the diameter of the 3D cell cultures was observed over time. A brighter central region could be detected in 3D cell cultures of more than 50,000 cells (D, G, J, K).

50,000 cell samples showed a brighter central region on the first day of light microscopy, while almost all of the larger 3D cell cultures (100,000 and 200,000 cells) showed a significantly brighter central region. For spheroids consisting of 100,000 and 200,000 cells, the non-spherical morphology could even be seen with the naked eye on day 1. For the group of 200,000 cells per 3D cell culture, we observed this morphology in some cases up to day 3.

Identification of the brighter central region as indentation in vital spheroids

To be sure that the visible brighter core region of the vital 3D cell cultures correlated with morphological characteristics, i.e. indentation in the central region, a measurement of the height profile was performed on both vital 3D cell cultures, with and without a clearly visible brighter central region. The convex height profile of a spheroid without a brighter central region can be clearly seen, as well as the concave height profile of a 3D cell aggregate with a brighter central region (Figure 2). These results clearly showed that the brighter inner regions of the 3D cell cultures corresponded to morphological indentations, which were accordingly referred to as 3D aggregates rather than spheroids.

SEM-analysis of the morphology of 3D cell cultures

In contrast to the light microscopic images of the 3D cell cultures shown in Figure 1, the SEM analysis allows a better evaluation of their morphology. Regardless of the number of cells organized in a 3D cell culture, we observed a time-dependent decrease in the size of the samples (Figure 3). It is noteworthy that the smallest 3D cell cultures (10,000 cells) already showed an almost spherical morphology but also a little bit lens-shaped morphology on day 1, whereas all larger 3D cell cultures exhibited a clearly visible indentation on day 1. By day 2 after seeding, 3D cell cultures consisting of 50,000 cells underwent reorganization and condensation, resulting in an almost spherical morphology (Figure 3E). The condensation and reorganization of the cells organized in 3D cell cultures is indicated by the development of a smoother surface of the 3D cell culture due to intensified cell–cell contacts and a stronger adherence of the cells to each other. In contrast, the indentation or cavity of the largest 3D cell cultures (200,000 cells) persisted until day 3 (Figure 3L). From day 1 to day 2, a clear reorganization, folding or condensation of the larger 3D cell cultures, can be observed, leading to a clear reduction in size of both, the size of the 3D cell culture itself and the central cavity (Figure 3J, K, L).

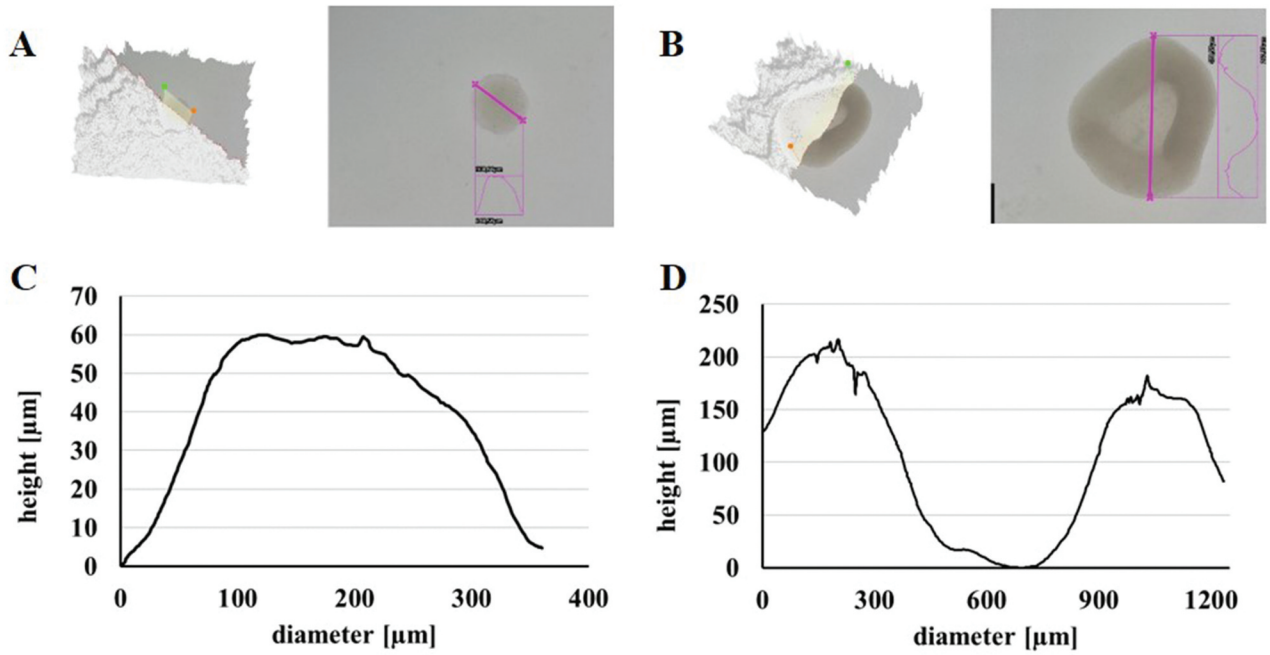

Figure 2. Height profiles of a vital spheroid of 10,000 cells on day 1 (A) and a vital 3D cell aggregate of 200,000 cells on day 1 (B) and corresponding results of the quantification of the height profiles (10,000 cells (C), 200,000 cells (D)). The convex height profile of the spheroid in (C) and the concave height profile of the 3D cell aggregate in (D) are clearly visible.

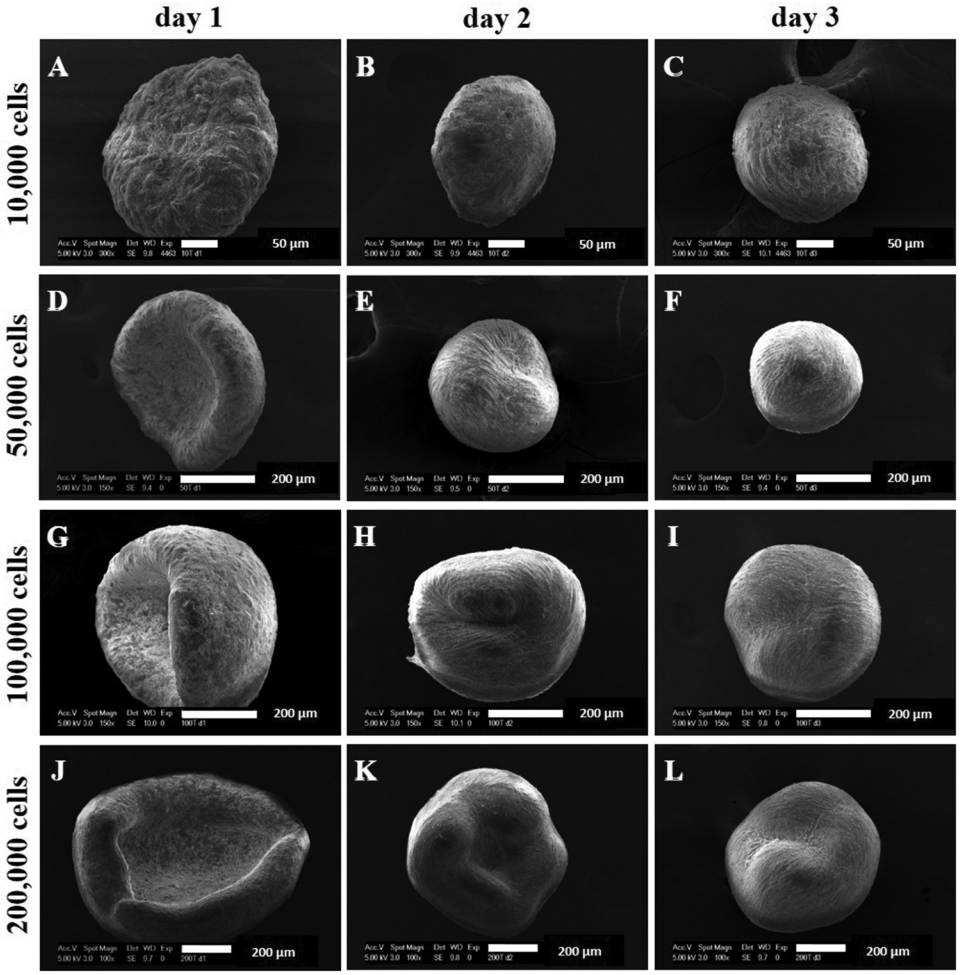

Figure 3. SEM images of GDA-fixed and dehydrated 3D cell cultures on day 1 (A, D, G, J), day 2 (B, E, H, K), and day 3 (C, F, I, L). 10,000 cells (A–C), 50,000 cells (D–F), 100,000 cells (G–I), and 200,000 cells (J–L) were seeded. The 3D cell cultures of 10,000 cells were almost uniformly round on the first day, but the larger ones showed distinct indentations on day 1.

Mathematical description of the size decrease of 3D cultures over time

The average size of the vital 3D cell cultures decreased continuously over time as shown in Figure 4. In all cases, the largest decrease in diameter was seen from day 1 to day 2 (16.7% (10 T); 19.8% (50 T); 14.7% (100 T); and 15.1% (200 T)). From day 1 to day 3, the decrease was only 7.9% (10 T), 8.7% (50 T), 11% (100 T), and 10% (200 T). It is worth mentioning that the low standard deviations impressively demonstrate the good reproducibility of the LOT.

To verify a correlation between decreasing size and time, the spheroid's diameters were normalized according to their diameter on day 1. Figure 5A shows that the relative shrinking over time seems to be independent of the cell number. To describe the shrinkage behavior, a mathematical equation was

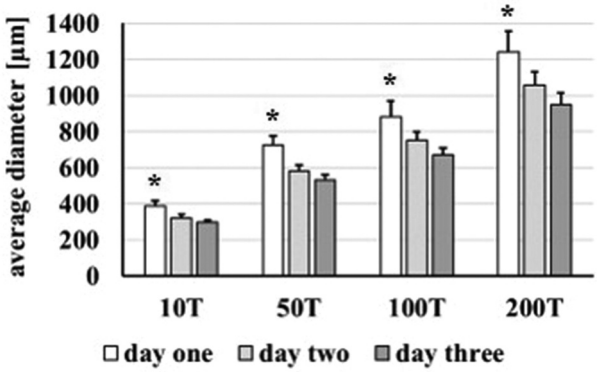

Figure 4. Evolution of the size (average diameter) of vital 3D cell cultures over time. * indicates significant differences ($p < 0.05$) of 3D cell cultures on day 1 compared with 3D cell cultures consisting of the same total number of cells on days 2 and 3. In each of five independent experiments, 15 3D cell cultures were analyzed.

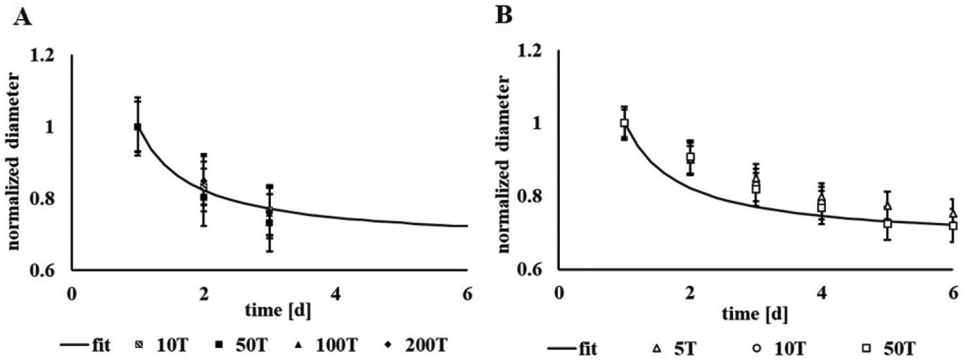

Figure 5. Decrease in normalized diameter of 3D cell cultures and theoretical model curve according to Equation (2). The experimental data shown in Figure 4 can be predicted very well with this equation (A), as well as data from an independent experiment with a different batch of NHDF and partially different cell numbers per spheroid (B).

established based on the normalized data of all spheroids. Assuming that the size of the spheroids will approach a lower limit >0 µm, an exponential decay function was used:

$$d = d_0 * \exp\left(-(t-1)\cdot\frac{0.39}{t}\right), t \text{ in days} \qquad (2)$$

The exponential part of the equation consists of a shift of the time $(t-1)$, because the data were normalized with the diameter on day 1. The constant 0.39 was obtained by fitting the data using the least squares error method (R^2 = 0.91). The fit describes the change of the diameter over time, as shown in Figure 5A very well.

Interestingly, even when using normalized results from an independent experiment (Metzger et al. 2021) with a different lot of NHDF and even smaller 3D cell cultures over a longer observation period up to day 6, it was possible to predict the diameter of these 3D cell cultures with this model (Equation 2) for t >4 days (Figure 5B). The difference of the model with the data can be explained with the sensitivity of the change of size during the first days. The interval between the size measurements (less or more than 24 h) has a major influence on the discrepancy between model and measurement for the first days. Nevertheless, the decrease in size of 3D cell cultures can be generally described by the proposed exponential decay function.

Quantification of number of spheroids

Since the number of round spheroids seemed to depend on the number of cells per 3D cell culture and age, we quantified the number in detail. Three groups of 3D cell cultures were evaluated as follows: vital, PFA-fixed, and GDA-fixed samples (after GDA-fixation, samples were dehydrated according to our standardized SEM protocol).

The LOT was able to generate almost 100% round spheroids of 10,000 cells on day 1 independent of any fixation, while seeding 50,000 cells per well resulted in only 80% round spheroids. Fixation with PFA further reduced the number of spheroids, an effect that was even more pronounced in the GDA fixed/dehydrated sample group. A higher number of seeded cells resulted in very few (100 T) or even no round spheroids (200 T) on day 1 (Figure 6A). On day 2, we observed a further increase in the number of vital and PFA-fixed spheroids of 50,000 cells up to 98.6%. After GDA fixation, we still saw a very low number of spheroids (50 T). Interestingly, the number of viable spheroids consisting of 100,000 or 200,000 cells increased significantly, reaching 96% for vital spheroids (100 T) (Figure 6B). The trend of an overall increase in the number of round spheroids continued on day 3 (Figure 6C). In summary, the number of spheroids increased with longer incubation time and decreased with higher number of seeded cells per well. Furthermore, fixation with PFA and especially fixation with GDA followed by dehydration reduced the number of spheroids and increased the number of 3D cell aggregates.

Discussion

Although much progress was made with standard 2D cell cultures since the first reports in the early 20th century, a new era in the development of cell culture began when simple 2D models gave way to more complex 3D cell culture models. Today, the scientific community accepts that cells can be better studied in 3D cell culture models, which reflect the dynamic state

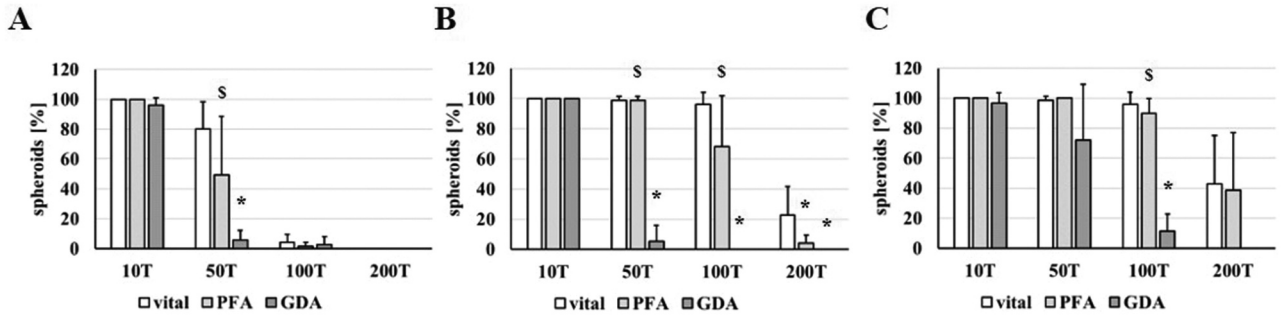

Figure 6. Number of round spheroids as a percentage of all 3D cell cultures. Evaluation of morphology of vital 3D cell cultures after fixation with PFA or fixation with GDA/dehydration was performed on day 1 (A), day 2 (B), and day 3 (C) after their generation by LOT. $ compared to GDA; * compared to vital; $p < 0.05$. In each of five independent experiments, 15 3D cell cultures were analyzed.

and physiological situation of cells in living tissues with more accurate precision (Zuchowska et al. 2024). Among other techniques, LOT is a powerful and at the same time simple method, that allows a consistent and highly reproducible generation of spheroids. However, the analysis of spheroid morphology by transmission light microscopy is very limited. The aim of this study was to describe the influence of the number of seeded cells and the incubation time as well as different fixation methods on the morphological development of NHDF 3D cell cultures.

In this study, the LOT once again demonstrated its high reproducibility: Independent of the number of cells seeded per well, exactly one spheroid was formed by scaffold-free self-assembly of the cells. The underlying principle of the local arrangement of cells within a spheroid can be explained by the so-called differential adhesion hypothesis (Steinberg 1970). According to this theory, the cells arrange themselves according to their surface and interfacial tensions in such a way that they assume an energetically favorable state, just like two immiscible liquids. The low standard deviations of spheroid size from our data indicate the high reproducibility of the LOT. Therefore, it is possible to generate spheroids of a defined size, which is crucial for studies in angiogenesis with hypoxia in mind (Heiss et al. 2015). Furthermore, the LOT offers a variety of possible variations, be it the generation of co-culture spheroids (Metzger et al. 2011; Walser et al. 2013; Dorst et al. 2014) or the combination of cells with functional microvascular fragments (Nalbach et al. 2021a, 2021b).

Despite all the advantages of spheroids, it is evident that microscopic analysis of spheroids is more challenging compared to 2D cultures. Standard transmission light microscopy is suitable for monitoring the formation of 3D cell cultures. However, this method provides only a 2D projection of the 3D sample, thus offering limited insight into the morphology of these 3D cell cultures and generally failing to discern indentations. In our previous studies, we never exceeded a number of 50,000 cells per spheroid, and not all of them showed a clearly visible brighter inner core during light microscopic analysis (Figure 1D). Therefore, the first step was to clarify the nature of this bright inner core. By measuring the height profiles with the Keyence microscope, we were able to identify the bright inner core region as an indentation (Figure 2). It is obvious that the formation of the indented morphologies depended on the number of seeded cells. The growth area of one well of a 96-well plate is only 34 mm^2. It is known that agarose forms a concave shape in the well (Friedrich et al. 2009). This concave shape of the agarose may help to attract cells to the center of the well, as we know from our previous work with 10,000 cell spheroids (Metzger et al. 2017). When a large number of cells are pipetted into a cavity, it is possible that the cells layer on top of each other at the edges of the agarose, an observation confirmed by microscopic observations after seeding: The sedimented cells were found positioned in different focal planes. The extreme indentation seen on day 1 (200,000 cells) is, therefore, an impression of the concave shape of the agarose, which gradually changes to a round shape through condensation and active cell migration.

The decrease in size of 3D cell cultures consisting of non-malignant cells is a well-known phenomenon and has already been described (Takezawa et al. 1993; Metzger et al. 2011, 2021; Grässer et al. 2018). We have shown that the size of individual cells forming the spheroid decreases due to 3D organization (Grässer et al. 2018). We hypothesized that condensation or reorganization of the spheroids could also be responsible for the shrinkage of the spheroids over time (Metzger et al. 2011). Considering our detailed SEM analysis of the 3D cell cultures (Figure 3), we assume that both mechanisms are responsible for the decreasing size of the spheroids over time. In particular, between days 1 and 2, the

spheroids appeared to undergo some kind of folding or condensation, leading to a reduction in the number of indentations, which at the same time led to a strong reduction in size (Figure 4). It was also striking that the small spheroids (10,000 cells) became darker over time (Figure 1), indicating a time-dependent condensation process in the spheroids.

Quantification of the ratio of viable spheroids to all 3D cell cultures was performed in conjunction with the photo documentation used to quantify spheroid size. Accordingly, the evaluation of the morphology of the 3D cell cultures had to be performed in the agarose-coated cavities of the 96-well plates and it was not possible to move or remove them to facilitate the analysis. This is important because these vital spheroids were incubated until day 3 and had to be handled very carefully. In contrast, it was possible to transfer fixed spheroids to a petri dish and gently move and rotate the samples with the tip of a pipette, which made the evaluation much easier. For the interpretation and evaluation of our results, it is important to know that two different quantification methods were used due to the experimental requirements described. Furthermore, in some cases it was difficult to decide whether a spheroid was almost round or had significant indentations during microscopic analysis. Nevertheless, some clear trends in the formation of round spheroids are evident:

Firstly, we observed a correlation between the number of seeded cells and the number of round spheroids: Seeding 10,000 spheroids resulted in 100% spheroids on the first day, while spheroids with a size of 200,000 cells had no round spheroids at all on the same day. This suggests that higher numbers of cells per spheroid correlate with a lower number of round spheroids. We hypothesize that cells sediment in layers on the agarose-coated wells, which are concave and form the indented 3D aggregates that we found in samples with high cell counts. It is clear that in case of seeding a low number of cells all cells sediment in the middle of the cavity, but that seeding a high number of cells leads to layered sedimentation upon the outer areas of the concave agarose. Therefore, the number of round spheroids decreases with increasing numbers of seeded cells.

Secondly, we observed an influence of time. As the spheroids aged, the number of round spheroids increased. This is consistent with our SEM images (Figure 3), which show a continuous condensation process over time. Specifically, the indentation of the 3D aggregates gradually diminishes over time and almost disappears on day 3 of the experiment. Furthermore, this condensation process is accompanied by a decrease in the size of the spheroids, as already discussed.

Thirdly, we observed that fixation of spheroids had an effect on the number of normal spheroids and 3D aggregates, and this depended on the type of fixation (PFA/GDA) too. For spheroids of 10,000 cells, we always evaluated approximately 100% spheroids. Only GDA fixation/dehydration resulted in a slight reduction in the number of round spheroids, indicating a high stability of smaller spheroids. For all other cell numbers, fixation with PFA and especially GDA followed by dehydration significantly decreased the number of round spheroids. It is known that the preparation of biological samples leads to a significant shrinkage of the samples compared to native samples (Katsen-Globa et al. 2016). With this in mind, it is very likely that the younger and larger spheroids lack stability, leading to the observed reduction of round spheroids after fixation. The basic chemical reaction behind aldehyde fixation is well known: the carbonyl groups of aldehydes are able to attack the nucleophilic amino groups of proteins, forming an intermediate Schiff base. Afterwards, this instable intermediate Schiff base is attacked by amino groups of another protein forming a stable covalent secondary amine linkage (Klockenbusch et al. 2012). Finally, the proteins are chemically cross-linked, which protects the biological sample against degradation. Concerning the influence on aldehyde fixation, it remains unclear which specific proteins are cross-linked in detail or if these linkages are within a single type of protein or between different proteins. However, it is very likely that fixation with aldehydes affects the structure of proteins somehow, as can be seen from the well-known reduction of immunohistochemical reactivity of epitopes and the need for antigen retrieval (O'Leary et al. 2009). It is possible that the observed significant decrease in the number of round spheroids after aldehyde fixation could be the result of cross-linking of proteins and a possible influence on the structure of proteins. This is most evident on day 1 after seeding of the cells, indicating that the structure of the spheroids is still unstable and is strongly affected by the chemical fixation.

Conclusion

The LOT is a powerful technique for generating spheroids with high reproducibility. Based on our findings, we recommend that spheroids of 100,000 cells or more, generated by LOT, should be cultured for at least 3 days to ensure a stable, spherical morphology before their use in downstream applications or fixation.

In addition, fixation with aldehydes had been shown to have a significant effect on the morphology of spheroids.

Acknowledgments

The authors are grateful for the excellent technical assistance of Daniela Sossong. The free version of DeepL Write was used to optimize the writing style.

Authors contributions

WM: conceptualization, methodology, writing and editing of the manuscript; EO: performing experiments, analyzing data, editing of the manuscript; LL: height profile measurement using the Keyence VHX 5000 microscope, editing of the manuscript, MH: methodology, editing of the manuscript; FK: mathematical description of the size decrease, editing of the manuscript; SA: conceptualization, editing of the manuscript, TP: conceptualization, editing of the manuscript.

Disclosure statement

No potential conflict of interest was reported by the authors.

Funding

This work was funded by the Deutsche Forschungsgemeinschaft (DFG- German Research Foundation)– project number 516192047.

Abbreviations

DMEM, Dulbecco's modified Eagle's medium; GDA, Glutardialdehyde; HMDS, Hexamethyldisilazane; LOT, Liquid overlay technique; NHDF, Normal Human Dermal Fibroblasts; PFA, Paraformaldehyde; PBS, Phosphate-buffered saline; SEM, Scanning electron microscopy.

ORCID

W. Metzger http://orcid.org/0000-0001-9668-4694
E. Oh http://orcid.org/0009-0005-0792-3662
L. Lemke http://orcid.org/0009-0001-1647-3983
M. Hannig http://orcid.org/0000-0003-0669-6881
F. Krull http://orcid.org/0000-0002-3704-8273
S. Antonyuk http://orcid.org/0000-0001-8068-1683
T. Pohlemann http://orcid.org/0000-0002-1288-0696

References

Achilli TM, Meyer J, Morgan JR. 2012. Advances in the formation, use and understanding of multi-cellular spheroids. Expert Opin Biol Ther. 12:1347–1360. https://doi.org/10.1517/14712598.2012.707181

Bloise N et al. 2024. Growing role of 3D in vitro cell cultures in the study of cellular and molecular mechanisms: short focus on breast cancer, endometriosis, liver and infectious diseases. Cells. 13:1054. https://doi.org/10.3390/cells13121054

Dorst N, Oberringer M, Grasser U, Pohlemann T, Metzger W. 2014. Analysis of cellular composition of co-culture spheroids. Ann Anat. 196:303–311. https://doi.org/10.1016/j.aanat.2014.05.038

Efremov YM et al. 2021. Mechanical properties of cell sheets and spheroids: the link between single cells and complex tissues. Biophys Rev. 13:541–561. https://doi.org/10.1007/s12551-021-00821-w

Fitzgerald KA, Malhotra M, Curtin CM, O'Brien FJ, O'Driscoll CM. 2015. Life in 3D is never flat: 3D models to optimise drug delivery. J Control Release. 215:39–54. https://doi.org/10.1016/j.jconrel.2015.07.020

Friedrich J, Seidel C, Ebner R, Kunz-Schughart LA. 2009. Spheroid-based drug screen: considerations and practical approach. Nat Protoc. 4:309–324. https://doi.org/10.1038/nprot.2008.226

Grässer U et al. 2018. Dissociation of mono- and co-culture spheroids into single cells for subsequent flow cytometric analysis. Ann Anat. 216:1–8. https://doi.org/10.1016/j.aanat.2017.10.002

Heiss M et al. 2015. Endothelial cell spheroids as a versatile tool to study angiogenesis in vitro. FASEB J. 29:3076–3084. https://doi.org/10.1096/fj.14-267633

Jennewein M et al. 2016. Two- and three-dimensional co-culture models of soft tissue healing: pericyte-endothelial cell interaction. Cell Tissue Res. 365:279–293. https://doi.org/10.1007/s00441-016-2391-0

Jensen C, Teng Y. 2020. Is it time to start transitioning from 2D to 3D cell culture? Front Mol Biosci. 7:33. https://doi.org/10.3389/fmolb.2020.00033

Katsen-Globa A, Puetz N, Gepp MM, Neubauer JC, Zimmermann H. 2016. Study of SEM preparation artefacts with correlative microscopy: cell shrinkage of adherent cells by HMDS-drying. Scanning. 38:625–633. https://doi.org/10.1002/sca.21310

Klockenbusch C, O'Hara JE, Kast J. 2012. Advancing formaldehyde cross-linking towards quantitative proteomic applications. Anal Bioanal Chem. 404:1057–1067.

Laschke MW, Menger MD. 2017. Life is 3D: boosting spheroid function for tissue engineering. Trends Biotechnol. 35:133–144.

Metzger W et al. 2011. The liquid overlay technique is the key to formation of co-culture spheroids consisting of primary osteoblasts, fibroblasts and endothelial cells. Cytotherapy. 13:1000–1012. https://doi.org/10.3109/14653249.2011.583233

Metzger W et al. 2014. Induction of osteogenic differentiation by nanostructured alumina surfaces. J Biomed Nanotechnol. 10:831–845. https://doi.org/10.1166/jbn.2014.1775

Metzger W et al. 2017. Evaluation of cell-surface interaction using a 3D spheroid cell culture model on artificial extracellular matrices. Mater Sci Eng C Mater Biol Appl. 73:310–318. https://doi.org/10.1016/j.msec.2016.12.087

Metzger W, Rösch B, Sossong D, Bubel M, Pohlemann T. 2021. Flow cytometric quantification of apoptotic and proliferating cells applying an improved method for dissociation of spheroids. Cell Biol Int. 45:1633–1643. https://doi.org/10.1002/cbin.11618

Nalbach L et al. 2021a. Microvascular fragment spheroids: three-dimensional vascularization units for tissue engineering and regeneration. J Tissue Eng. 12:20417314211035593.

Nalbach L et al. 2021b. Improvement of islet transplantation by the fusion of islet cells with functional blood vessels. EMBO Mol Med. 13:e12616. https://doi.org/10.15252/emmm.202012616

O'Leary TJ, Fowler CB, Evers DL, Mason JT. 2009. Protein fixation and antigen retrieval: chemical studies. Biotech Histochem. 84:217–221. https://doi.org/10.3109/10520290903039086

Rescigno F, Ceriotti L, Meloni M. 2021. Extra cellular matrix deposition and assembly in dermis spheroids. Clin Cosmet Investig Dermatol. 14:935–943. https://doi.org/10.2147/CCID.S316707

Saraswathibhatla A, Indana D, Chaudhuri O. 2023. Cell-extracellular matrix mechanotransduction in 3D. Nat Rev Mol Cell Biol. 24:495–516. https://doi.org/10.1038/s41580-023-00583-1

Später T et al. 2022. Vascularization of microvascular fragment isolates from visceral and subcutaneous adipose tissue of mice. Tissue Eng Regen Med. 19:161–175. https://doi.org/10.1007/s13770-021-00391-8

Steinberg MS. 1970. Does differential adhesion govern self-assembly processes in histogenesis? Equilibrium configurations and the emergence of a hierarchy among populations of embryonic cells. J Exp Zool. 173:395–433. https://doi.org/10.1002/jez.1401730406

Takezawa T, Mori Y, Yonaha T, Yoshizato K. 1993. Characterization of morphology and cellular metabolism during the spheroid formation by fibroblasts. Exp Cell Res. 208:430–441. https://doi.org/10.1006/excr.1993.1265

Unger C et al. 2014. Modeling human carcinomas: physiologically relevant 3D models to improve anti-cancer drug development. Adv Drug Deliv Rev. 79–80:50–67. https://doi.org/10.1016/j.addr.2014.10.015

Walser R et al. 2013. Generation of co-culture spheroids as vascularisation units for bone tissue engineering. Eur Cell Mater. 26:222–233. https://doi.org/10.22203/eCM.v026a16

Zanoni M, Pignatta S, Arienti C, Bonafe M, Tesei A. 2019. Anticancer drug discovery using multicellular tumor spheroid models. Expert Opin Drug Discov. 14:289–301. https://doi.org/10.1080/17460441.2019.1570129

Zuchowska A, Baranowska P, Flont M, Brzozka Z, Jastrzebska E. 2024. Review: 3D cell models for organ-on-a-chip applications. Anal Chim Acta. 1301:342413. https://doi.org/10.1016/j.aca.2024.342413